# An Empirical Study of the Achievable Rates of Several Indoor Network-MIMO Techniques

Rodolfo Feick, *Senior Member, IEEE,* Milan S. Derpich, *Member, IEEE,* Reinaldo A. Valuenzuela, *Fellow, IEEE,* Héctor Carrasco, Luciano Ahumada, *Member, IEEE,* Howard Huang, *Senior Member, IEEE,* Chris T. K. Ng, *Member, IEEE*, and Pablo Arancibia

***Abstract*—This paper presents an empirical study of the achievable data rates of network multiple-input multiple-output (MIMO) techniques including zero-forcing (ZF), zero-forcing dirty paper coding (ZF-DPC) and dirty paper coding (DPC) using actual 4-by-4 indoor wireless channel measurements at 3.5 GHz. Their performances are contrasted with those of conventional techniques, in which either the base stations are not coordinated (NC), or their interference is avoided using frequency division (FD) multiplexing. The measurements were taken in aisle-to-office and large unobstructed hall scenarios. The study of these results reveals that, at high signal-to-noise ratios (*SNR*s), DPC and ZF-DPC can yield more than a three-fold increase in attainable data rates when compared to NC and FD. The gains obtained using ZF are smaller, but still significant. At low *SNR*s the system is noise-(rather than interference-) limited, and only DPC exhibits gains. The evaluations in this paper also show that collaborative systems such as DPC can benefit from interference-prone environments to yield increased transmission capacity. With regard to the propagation channel, the classical log-normal plus Rayleigh/Ricean fading model, with parameters fitted to the scenario type, was found to be good at predicting the statistics of the achievable data rates of all the strategies considered.**

***Index Terms*—Wireless communication, MIMO, channel characterization and modeling, performance analysis.**

## I. Introduction

THERE is an ever increasing demand for high data rates in homes and offices with all the mobility provided by wireless technology. Since growing numbers of users are to be served within confined spaces, the performance of practical indoor wireless communications systems is expected to be limited, increasingly often, by interference [1]–[3]. Therefore, in order to improve (or even maintain) high data rates, it will become necessary to make use of communication techniques capable of exploiting the coupling between the various propagation links within a given service scenario so as to reduce interference and increase received signal power.

Manuscript received January 24, 2010; revised June 26, 2010; accepted September 4, 2010. The associate editor coordinating the review of this paper and approving it for publication was M. Tao.

R. Feick, M. S. Derpich, and H. Carrasco are with the Electronics Engineering Department, Universidad Técnica Federico Santa María, Valparaíso, Chile (e-mail: {rodolfo.feick, milan.derpich, hector.carrasco}@usm.cl).

R. Valenzuela, H. Huang, and C. Ng are with the Wireless Communications Research Department, Bell Labs, Alcatel-Lucent, NJ, USA (e-mail: {reinaldo.valenzuela, Howard.Huang, chris.ng}@alcatel-lucent.com).

L. Ahumada is with the Esc. Ing. Informática, Univ. Diego Portales, Santiago, Chile (e-mail: luciano.ahumada@udp.cl).

P. Arancibia is with Defontana Chile (e-mail: p.trecaman@gmail.com).

This work was supported by FONDECYT project Nrs. 1095018, 3100109, 1095139, and CONICYT project ACT-53.

Digital Object Identifier 10.1109/TWC.2011.122010.100102

This management of the interference produced by *access points* (APs) and users can be achieved by means of coordination. Having all APs operating in a coordinated fashion turns the set of users and APs into a network *multiple-input multiple-output* (MIMO) system, and the downlink communication medium into a *MIMO broadcast channel* (MIMO-BC). Network-MIMO systems hold the potential of eliminating interference in a MIMO-BC, greatly increasing bandwidth efficiency in multi-AP wireless systems [3], [4].

Several strategies have been proposed in the literature to take advantage of the high interconnectivity between several APs and a group of users that is often encountered in MIMO-BC scenarios. The technique called *dirty paper coding* (DPC) [5], [6] has been shown to be capacity-achieving in this setting, and thus it is optimal [7], [8]. DPC is a nonlinear precoding technique that requires full knowledge of *channel state information* (CSI) at the transmitter.

The high implementation complexity of DPC suggests the need to consider other simpler, near-optimal MIMO-BC transmission schemes. One such technique, commonly referred to as *zero-forcing-DPC* (ZF-DPC) [9], [10], achieves sum rates close to those of DPC with smaller computational complexity. In ZF-DPC, part of the interference is removed by linearly combining the signals intended for all users so as to effectively obtain, from end to end, a lower triangular channel matrix. The triangularization of the channel matrix, which requires perfect CSI at the transmitter side, makes it possible to avoid part of the interference. The effect of all remaining interference is eliminated by applying DPC in a sequential fashion.

Another suboptimal technique, simpler than DPC and ZF-DPC, is *zero-forcing* (ZF) beamforming as described in [11]–[13]. Zero-forcing is an entirely linear preprocessing strategy. In this case, APs have perfect CSI and cooperate to eliminate interference for all users, yielding an effectively diagonal channel matrix between transmitted data flows and users.

Simpler strategies to attain downlink communication in a MIMO-BC are obtained if each AP serves a single user and its CSI is limited to the radio link to that user only. In our work, we consider two possible approaches. The first one is *frequency division* (FD), that is, splitting the available spectrum into disjoint frequency bands, each one allocated to a single AP-user pair, with each AP transmitting at full power. The second approach, which will be referred to as the *non-coordinated* (NC) strategy, is to let each AP transmit at full power using all the spectrum available, thus accepting that interference from other users will limit data rates as transmission

power increases. The simpler FD and NC schemes in general have inferior performances than those of DPC and ZF-DPC. On the other hand, the former strategies impose the minimum possible backhaul load, since each AP needs to know only the data intended for (and the CSI related to) the user it is serving. There exist other strategies for downlink communication in a MIMO-BC that do not require coordination among APs and whose performance is under certain conditions better than that of FD and NC, such as *fractional frequency reuse* (FFR) [14]. Although it is known that in some specific cases FFR outperforms FD (see, e.g., [14], [15]) our objective here is only to provide a few simple baseline systems as a reference for comparison. It is understood that whichever is the choice, different propagation conditions may favor different baseline strategies.

The performance evaluation of diverse network-MIMO techniques for simulated channels has been treated in various works [11], [16]–[19]. This has included the assumption of log-normal plus Rayleigh fading, and the use of the Wyner model [20]–[25]. The effect of limited backhaul capacity between APs in overall performance is assessed in [26]–[28].

Regarding the channel model, it may be reasonable to assume that small-scale fades are independent for each channel when antennas are several wavelengths apart, but this may not hold for shadow fades. Several articles report on the correlation of fades in different locations of transmit and receive antennas [29]–[34]. To what extent such correlation may affect the network-MIMO channel, based on widely separated base station antennas, is not self-evident. To the best of our knowledge, no empirically based results in support of the assumption that a network-MIMO channel is equivalent to a collection of independent SISO channels have been published.

The fact that in network MIMO all APs can act in a coordinated fashion taking advantage of CSI, generates two related sources of capacity improvement. Interference between AP-user pairs can be reduced and, at the same time, the total received signal power at each user terminal can be increased. Since these effects depend on the degree of connectivity (or, conversely, isolation), this raises the question of how much performance improvement can be expected for a given type of deployment scenario.

In this paper, we evaluate and compare the maximum data rates achievable by the DPC, ZF-DPC, ZF, FD and NC strategies, for measured as well as simulated 4-by-4 MIMO indoor channels, under a *per antenna power constraint* (PAPC). These rates were all calculated under the assumption of perfect CSI at the transmitter. Although this would be hard to attain with currently available technology, the results serve as a comparison basis, being the best performance achievable under equally idealized conditions for all schemes. Channel measurements were obtained for two representative scenarios: aisles with offices alongside them, and large halls. A single slope path-loss model with log-normal shadow fading and Rice/Rayleigh small scale fades [35], was found to be adequate in all the scenarios for the distances at which measurements were taken. With regard to achievable data rates, we found that at high *SNR*s (in the range of 30 dB), DPC and ZF-DPC achieve about a three-fold gain when compared to NC or FD. The gains of ZF are somewhat smaller, depending on the scenario, but still quite significant. A particularly interesting finding is that both DPC schemes not only are able to effectively mitigate the effect of interference but also in some cases can exploit low isolation between AP-user pairs, to yield higher data rates than in scenarios with greater natural isolation. As would be expected, at low *SNR*, where interference is not the dominant limitation on capacity, the gain over the non-coordinated systems decreases. Our study also reveals that the log-normal plus Rice/Rayleigh fading model is accurate at predicting the statistics of the maximum rates achievable by each of the network-MIMO strategies considered, when the model parameters are selected according to the type of scenario. Thus, an indoor MIMO channel described as a collection of independent SISO channels, would yield similar conclusions to those of our empirically based study, provided that the proper model parameters are used. However, rather than justifying what could have been deemed as somewhat arbitrary choices of parameters to illustrate the achievable benefits of a coordinated system, we decided to use actual measured channel data from typical indoor scenarios to validate our comparison. In the following sections we describe our measurement procedures and the empirical results obtained from them.

## II. Measurement Setup and Scenarios

### A. Measurement Setup

In all measurements, the custom-built channel sounder used consisted of a single channel transmitter and a 4-channel receiver operating at 3.5 GHz for narrowband measurements. The single transmit antenna was placed at locations that would in practice correspond to possible positions of a user. Four receive antennas, one per AP, were placed at the positions typical of AP locations. The antennas used for transmission and reception were omnidirectional coaxial dipoles, vertically polarized. The transmit antenna was mounted on a 50-cm long rotating arm and moved stepwise under computer control in 6-degree increments.

In all scenarios, measurements were taken at night in the absence of pedestrian movement. For each of the 5 scenarios (3 aisle-to-office and 2 halls), more than a 1000 complex 1-by-4 channel vectors were collected, each vector containing the complex gains from a user location to the four APs.

The single conversion receiver generates 4 channel outputs at 10 kHz. The sampled receiver output sequences were converted into a vector of 4 complex channel gains using the Fast Fourier Transform (FFT). Phase coherence was achieved by locking the transmitter and receiver oscillators to GPS disciplined sources. Exact synchronization of sampling intervals produces data sequences corresponding to an integer number of periods of the 4 sinewave outputs, which allowed FFT processing without the need for windowing. For each position of the transmit antenna, the 4 channel outputs were simultaneously sampled for 1 second, and the total interval was partitioned into 100 non-overlapping subintervals of 10 ms each. This allowed us to verify the consistency of our measurements which should only differ as a consequence of receiver noise. Since the MIMO capacity depends on the

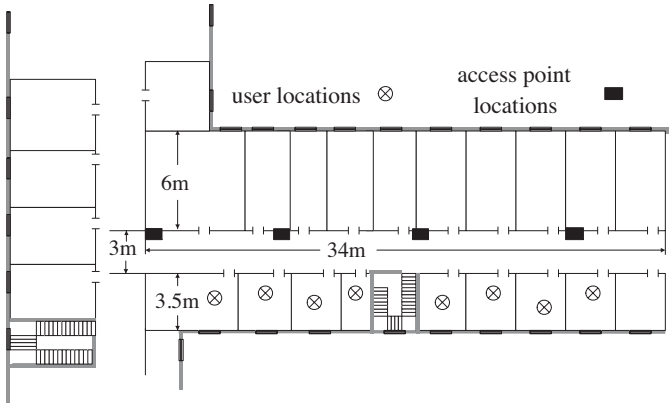


Fig. 1. Diagram of scenario aisle-to-office 1.

relative rather than the absolute phases of the channels, we calculated phase differences with respect to one of the channels, arbitrarily chosen as a reference. In all our measurements, the ratio between the average gain (magnitude) and its rms fluctuation, calculated over the sequence of 100 measurements, exceeded 20 dB. Thus by averaging our measurements, we further reduced the effect of the measurement noise.

### B. Measured Scenarios

We performed measurements in two types of scenarios which we considered relevant and where, as our data subsequently confirmed, different propagation behaviours are to be expected. These scenario types are as follows:

*1) Aisle-to-office Scenarios:* Channel measurements were carried out in three different aisle-to-office scenarios. In all cases the building was a steel reinforced concrete structure with interior divisions made of wood and particleboard. For these scenarios, the four receive antennas were wall-mounted at a 2.5 m-height along straight aisles, with a 10-cm separation from the particleboard interior walls. Adjacent AP antennas were separated by approximately 8 m. The transmit antenna was placed at desktop height inside various offices and laboratories adjacent to the aisle. These are *non-line-of-sight* (NLOS) scenarios. The distances between the transmit antenna and the 4 receive locations ranged from 3 to 25 m. The locations of transmit and receive antennas for scenario aisle-to-office 1 is indicated schematically in Fig. 1. In this figure, the rectangles and circles represent AP and user locations, respectively. The other two scenarios of this type had similar topologies. In each office, measurements were obtained placing the rotating arm on three or four different user locations, more than 1-m apart from one another, as space would allow (for simplicity, only one of these user locations per office is shown in Fig. 1).

*2) Large Hall Scenarios:* We obtained measurements from two large halls. The first one, hall-1, was a 53-m $\times$ 14-m, glass-roofed central hall, about 7-m high, with concrete floor and several lateral aisles leading to offices and classrooms on two floors. This hall is built with steel beams with concrete walls separating the hall from the adjacent spaces. The four receive antennas were located at the corners of an imaginary rectangle, with each antenna at approximately 10 cm from a wall on the hall, at heights of about 2.5 m. The transmitter rotating arm was placed in 38 different positions over a grid of locations within the rectangle formed by the receive antennas. This is a *line-of-sight* (LOS) scenario, in which link lengths ranged from 4 to 26 m.

The second hall scenario, hall-2, was a 17-m $\times$ 23-m gymnasium with wooden floor and concrete walls. The four receive antennas were placed as in hall-1, while the rotating arm was placed in 43 different positions over a grid inside the gymnasium. Transmitter-receiver distances varied from 5 m to nearly 24 m.

## III. Statistics of Measured Data and Model Fitting

Before using the obtained channel measurements to calculate the data rates achievable with network-MIMO techniques, we describe the observed statistical properties of the fades in each scenario.

The measured channel gains proved to be consistent with what has been reported in the literature for similar scenarios [35]–[42]. We found that log-normal shadow fading combined with Rayleigh or Ricean small-scale fades resulted in an excellent model fit to our narrowband measurements, provided the model parameters are adjusted to the measured data. The statistics of each type of fading are described below.

### A. Small-scale fading

For each wireless link, small-scale fading statistics were analyzed by studying the 60 channel gain measurements corresponding to a single turn of the rotating arm. As expected, in all aisle-to-office scenarios, these channel gains showed fading statistics that were well described by a Rayleigh distribution. This is consistent with a NLOS situation [35].

In the scenarios hall-1 and hall-2, these gains fit a Rice distribution with K-factor between 0 and 3. It is worth noting that despite the fact that these scenarios are LOS, they are, as the previous ones, characterized by strong multipath propagation, although to a lesser extent. In all scenarios, the channel phases associated with each angular position of the rotating arm were uniformly distributed and uncorrelated.

### B. Large-scale fading

The large-scale fading statistics were obtained by calculating, at different locations, the averages of the channel gains over an arm rotation. The statistics of these average gains were well described by a log-normal distribution. More precisely, for each link distance $d$, the path-loss, $L(d)$ in dB, corresponding to each rotation-averaged channel gain followed the behaviour of a random variable of the form

$$L(d) = L_{ref} + 10n\log_{10}(d/d_{ref}) + X_\sigma, \qquad (1)$$

where $n \in \mathbb{R}^+$ is a path-loss exponent, $X_\sigma$ is a zero-mean Gaussian random variable with variance $\sigma^2$ and $L_{ref}$ is the path loss in dB at $d = d_{ref}$, which we chose as 1 m. For each measured scenario, the model described by (1) was fitted to 80 measured large-scale path losses, finding $L_{ref}$ and $n$ by linear regression, and then setting $\sigma^2$ as the empirical variance of $L(d) - L_{ref} - 10n\log_{10}(d/d_{ref})$. The values of $n$ and $\sigma$ so obtained are listed in Table I. For each scenario type, a

TABLE I
PARAMETERS OF (1) FITTED TO MEASURED SCENARIOS.

| Scenario | $Lref$ [dB] | $n$ | $\sigma$ [dB] |
|---|---|---|---|
| Aisle-to-office 1 | 39.8 | 3.7 | 3.1 |
| Aisle-to-office 2 | 50.3 | 2.9 | 3.5 |
| Aisle-to-office 3 | 42.9 | 3.0 | 2.9 |
| **All aisle-to-office scenarios** | **45.6** | **3.1** | **4.1** |
| Hall 1 | 50.3 | 1.3 | 2.1 |
| Hall 2 | 51.5 | 1.2 | 2.2 |
| **All hall scenarios** | **50.8** | **1.3** | **2.1** |

row in boldface contains the model parameters resulting from combining all data of its corresponding scenarios.

It is worth mentioning that no evidence of a "break point" in the path-loss exponent was found from the measurements. More precisely, no multi-slope models [43] were found to provide a better match (in a least-squares sense) to our empirical data. This is consistent with what has been reported before for short-range indoor scenarios [44], [45].

It was also found that the correlation between the shadow fades in the links between a transmitter antenna and any two receiving antennas was, in all cases, below $0.26$ (in modulus). This was true even when the two receiving antennas (in all cases several meters apart) were seen by the transmitter at an angle narrower than 10 degrees.

## IV. BRIEF REVIEW OF NC, FD, ZF, ZF-DPC AND DPC

In this section we present a brief review of the transmission techniques to be evaluated in Section V and their relation to the channel model.

### A. Channel Model

A general MIMO wireless downlink narrowband channel between $M$ single-antenna APs and $K$ single-antenna users can be represented by a $K \times M$ complex valued matrix $\mathbf{H}$. Denoting the vector of signals transmitted by the $M$ access points by $\mathbf{x} \in \mathbb{C}^M$, the vector of received signals $\mathbf{y} \in \mathbb{C}^K$ can be written as

$$\mathbf{y} = \mathbf{H}\mathbf{x} + \mathbf{n}, \tag{2}$$

where the noise vector $\mathbf{n} \in \mathbb{C}$ has i.i.d. circularly symmetric complex Gaussian elements with variance $N$. Notice that $h_{k,m}$, the element in the $k$-th row and $m$-th column of $\mathbf{H}$, is the narrow-band channel gain between the $m$-th AP and the $k$-th user. Notice also that no joint processing of the output of the MIMO channel is allowed, since it is assumed that cooperation between users is not practical.

For the three network-MIMO strategies considered in this work, $\mathbf{x}$ can be constructed as

$$\mathbf{x} = \mathbf{W}\mathscr{T}\mathbf{u}, \tag{3}$$

where the $k$-th element in the vector $\mathbf{u} \in \mathbb{C}^K$ is the information-bearing signal intended for the $k$-th user, $\mathbf{W} \in \mathbb{C}^{M\times K}$ is a linear preprocessing matrix, and $\mathscr{T} : \mathbb{C}^K \to \mathbb{C}^K$ is either a non-linear transformation, in the case of DPC schemes, or the identity matrix, in the case of ZF. We note that an element of $\mathbf{x}$ can be a function of two or more user signals only if the APs are able to operate cooperatively. Following standard practice, we will assume that the elements of $\mathbf{u}$ are independent zero-mean complex Gaussian random variables with variances

$$p_k \triangleq \mathrm{E}\left[u_k u_k^*\right]$$

for $k = 1, 2, \ldots, K$. Thus, (2) can be written as

$$\mathbf{y} = \mathbf{H}\mathbf{W}\mathscr{T}\mathbf{u} + \mathbf{n}. \tag{4}$$

We will assume that the APs are subject to a PAPC of the form

$$\sigma^2_{\mathrm{x}_m} \le P, \quad \forall m = 1, 2, \ldots, M, \tag{5}$$

where $\sigma^2_{\mathrm{x}_m}$ is the variance of the $m$-th element of $\mathbf{x}$, for some maximum power $P \ge 0$. All channel matrices considered in the sequel are 4-by-4, that is, $K = M = 4$, restricting our analysis to four users served simultaneously by four APs.

### B. Non-Coordinated System (NC)

We include NC and FD as baseline strategies, against which to compare the other three (network-MIMO) schemes. In the case of NC, each AP serves a single user, and all APs operate without coordination, transmitting at maximum power over the same frequency band. In terms of the model (4), this amounts to restricting $\mathbf{W}$ to be a diagonal matrix, or any row or column permutation of it. Since the user signal variances $\{p_k\}$ can be chosen freely, there is no loss in generality in assuming for this case that $\mathbf{W} = \mathbf{I}$, where $\mathbf{I}$ is the identity matrix. With this, the sum rate achievable with an NC system is readily found to be

$$R_{\mathrm{NC}}(P) = \sum_{k=1}^{K} \log_2\left(1 + \frac{P|h_{k,k}|^2}{N + P\sum_{m\neq k}|h_{k,m}|^2}\right) \text{ [bps/Hz]}. \tag{6}$$

In this expression, $P|h_{k,k}|^2$ is the power of the signal $u_k$ as received by its intended user. On the other hand, $P\sum_{m\neq k}|h_{k,m}|^2$ represents the interference affecting the $k$-th user, produced by the APs serving all the other users.

### C. Frequency Division Scheme (FD)

In this case, each AP transmits at full power using a fraction of the available spectrum. We will assume that this spectrum is partitioned into $K$ adjacent non-overlapping equal-width bands. Therefore, assuming the same total bandwidth as for NC, the maximum achievable rate of FD is trivially given by

$$R_{\mathrm{FD}}(P) = \frac{1}{K}\sum_{k=1}^{K} \log_2\left(1 + \frac{|h_{k,k}|^2 P}{N/K}\right) \quad \text{[bps/Hz]}. \tag{7}$$

### D. Zero-Forcing (ZF)

The idea in ZF is to eliminate, in the downlink, all interference produced by the APs. To do this, the matrix $\mathbf{W}$ in (4) is chosen as[1] $\mathbf{W} = \mathbf{H}^{-1}$. This requires all APs to have CSI and each of them to process the signals intended to all users.

[1]In general, since $\mathbf{H}$ may be rectangular or singular, $\mathbf{W}$ is typically chosen as the pseudo-inverse of $\mathbf{H}$. However, since in our study $\mathbf{H}$ is square and all its realizations were non-singular, we will simply use the inverse of $\mathbf{H}$.

In this case, the highest sum rate (bits per second per Hz) achievable under a PAPC $P$ is readily found to be [46]

$$R_{\text{ZF}}(P) = \max_{\{p_k\}} \sum_{k=1}^{K} \log_2\left(1 + \frac{p_k}{N}\right) \quad \text{[bps/Hz]}, \tag{8}$$

where the signal powers $\{p_k\}$ are subject to

$$0 \leq p_k, \quad k = 1, 2, \ldots, K \tag{9a}$$

$$0 \leq \sum_{k=1}^{K} |w_{m,k}|^2 p_k \leq P, \quad m = 1, 2, \ldots, M \tag{9b}$$

and where $w_{m,k}$ denotes the entry on the $m$-th row and $k$-th column of $\mathbf{W}$. The optimization problem defined by (8) and (9) has been shown to be convex in [11]. Therefore, a global maximum for the right-hand side of (8) can be obtained numerically using standard convex optimization methods [47]. Notice that the solution to (8) subject to (9) will, in general, yield antenna transmit powers $\sigma^2_{\mathrm{x}_m} < P$ for one or more $m \in \{1, 2, \ldots, M\}$. ZF is known to perform poorly at low SNR but it is easy to improve its achievable rate under such conditions by choosing W as a regularized inverse of H instead of its true inverse [48]. We denote this variant of ZF as *regularized zero-forcing* (RZF).

### *E. Zero Forcing Dirty Paper Coding (ZF-DPC)*

This MIMO-BC technique was first proposed in [9] and then further studied in [10]. The idea behind ZF-DPC is to utilize the linear preprocessing matrix $\mathbf{W}$ to assure that the $k$-th user receives no interference from the signals $u_j$, for all $j > k$, and then use DPC to avoid the effects of the remaining interference. More precisely, $\mathbf{W}$ is chosen so as to obtain

$$y_k = g_{k,k} v_k + n_k + \sum_{j=1}^{k-1} g_{k,j} v_j, \tag{10}$$

where $g_{k,j}$ are the elements of some lower-triangular matrix $\mathbf{G}$ and $v_k$ is the $k$-th element of the vector

$$\mathbf{v} \triangleq \mathscr{T}\mathbf{u},$$

see (3). In [10] and [49], this is achieved by choosing

$$\mathbf{W} = \mathbf{Q}, \tag{11}$$

where $\mathbf{Q}$ is the unitary matrix in a QR decomposition of $\mathbf{H}^H$, i.e., $\mathbf{H} = (\mathbf{QR})^H$, with $\mathbf{R}$ being an upper triangular matrix and $(\cdot)^H$ denoting the conjugate transpose operator. Choosing $\mathbf{W}$ as in (11), we have that

$$\mathbf{y} = \mathbf{HWv} + \mathbf{n} = \mathbf{R}^H\mathbf{v} + \mathbf{n} \tag{12}$$

which attains the interference-avoidance outcome described by (10) with $\mathbf{G} = \mathbf{R}^H$. If $\mathbf{H}$ is invertible (as is the case in all the channel matrices considered in this work), then all matrices $\mathbf{R}$ satisfying this factorization differ only by a sign inversion in any subset of their rows.[2] Therefore, in our case, the absolute value of each element of $\mathbf{R}$ (and thus of $\mathbf{G}$ as well) is fixed once $\mathbf{H}$ is known.

[2]This is a direct consequence of the well known fact that, for a non-singular square matrix $\mathbf{H}$, there exists a unique QR factorization $\mathbf{H}^H = \mathbf{QR}$ in which all the elements in the main diagonal of $\mathbf{R}$ are positive, see, e.g., [50].

In ZF-DPC, the effect of the interference represented by the sum at the right end of (10) is avoided by employing *dirty paper coding* (DPC) [5]. The latter requires having, at the transmitting end, perfect CSI as well as full knowledge of all user signals. After applying DPC and transmitting the result through the channel (10), each $u_k$ is decoded as if there had been no interference at all [5]. Therefore, the achievable sum-rate of ZF-DPC is given by

$$R_{\text{ZF-DPC}}(P) = \max \sum_{k=1}^{K} \log_2\left(1 + \frac{|r_{k,k}|^2 p_k}{N}\right) \text{[bps/Hz]}, \tag{13}$$

where $r_{k,k}$ are the elements in the diagonal of $\mathbf{R}$ and where the maximization is over all row permutations of $\mathbf{H}$ and power allocations $\{p_k\}$ that satisfy the PAPC (9) for each permutation. Notice that in this case the scalars $w_{m,k}$ in (9) are the elements of preprocessing matrix $\mathbf{W}$ defined in (11) for the row-permuted matrix $\mathbf{H}$.

It is easy to show that the optimization problem defined by (13) and (9) is also convex for each permutation. To see this, it suffices to notice that the change of variables $\bar{p}_k \triangleq p_k/|r_{k,k}|^2$ and $\bar{w}_{m,k} \triangleq w_{m,k}|r_{k,k}|^2$ yields the optimization problem defined by (13), (9) equivalent to (8), (9).

The performance of ZF-DPC has been evaluated using simulated channel data in [10], under a sum power constraint, and in [49], under a PAPC. In both cases, ZF-DPC was shown to be superior to ZF and various non-cooperative MIMO strategies.

### *F. Dirty Paper Coding (DPC)*

Although the practical implementation of DPC still awaits specific code designs, we use this technique as an ultimate upper bound for the achievable data rates in each scenario.

In DPC, no a-priori restriction is imposed on the preprocessing matrix $\mathbf{W}$. Here, the signal intended for user 1, $u_1$, is transmitted by (possibly) all APs as if there were no other signals being transmitted, i.e., $v_1 = u_1$. In contrast, the data aimed at user 2 is encoded using DPC into $v_2$, exploiting the fact that all APs have full CSI, which together with having knowledge of $u_1$, allows avoiding its interfering effect. The resulting signal is then sent using (possibly) all APs as well. Notice that, by doing this, $v_2$ is added to the signal received by user 1 as interference. A similar process is employed to successively encode the data for the remaining users, utilizing previously encoded signals as known interference. In this setting, the signal $v_k$ with power $p_k$ reaches all APs through the $k$-th column of $\mathbf{W}$, thus arriving at the corresponding user with power $p_k \left|\sum_{\ell=1}^{K} h_{k,\ell} w_{\ell,k}\right|^2$ (as before, $w_{\ell,k}$ denotes the entry on the $\ell$-th row, $k$-th column of $\mathbf{W}$). Therefore, the maximum rate achievable with this technique is [51]

$$R_{\text{DPC}}(P) = \max \sum_{k=1}^{K} \log_2\left(1 + \frac{p_k \left|\sum_{\ell=1}^{K} h_{k,\ell} w_{\ell,k}\right|^2}{N + \sum_{j=k+1}^{K} p_j \left|\sum_{\ell=1}^{K} h_{k,\ell} w_{\ell,j}\right|^2}\right) \text{[bps/Hz]}, \tag{14}$$

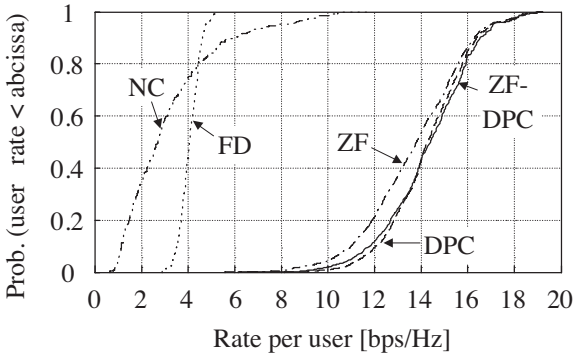


Fig. 2. CDF plots of rate per user, obtained when NC, FD, ZF, ZF-DPC and DPC achieve their maximum sum-rates, under the power constraint $P = 20$ dBm, from empirical channel measurements taken in scenario aisle-to-office 1.

where the maximum is taken over all permutations of the rows of $\mathbf{H}$ and over all matrices $\mathbf{W} \in \mathbb{C}^{K\times K}$ and powers $p_k$ satisfying (9) for each permutation. An efficient method to numerically solve the optimization problem posed by (14) has been proposed in [52]. This is the method we used to evaluate $R_{\text{DPC}}(P)$ for the measured and simulated channel data.

In the next section we use the above expressions to compare the performance of the various schemes in realistic indoor environments. We use both actual measured channel matrices as well as channel matrices generated by the model obtained from our measurements.

## V. Rate Evaluation and Comparisons

In this section we evaluate the maximum sum rates of NC, FD, ZF, ZF-DPC and DPC as described respectively by (6), (7), (8), (13) and (14), subject to the PAPC (9), for the measured channel matrices obtained in all scenarios. We then repeat the sum-rate evaluation using channel matrices generated by the model (1), using the appropriate parameters as derived from our measurements. For the aforementioned transmission schemes, we calculate the per-user rates at specific availabilities, i.e., the maximum per-user rate that is guaranteed to be met or exceeded with some given probability.

We further assume that the scheduler in this system is perfectly unbiased in that, on average, all users are served an equal amount of time. At the same time, our procedure of AP-to-user associations is designed to avoid combinations that will yield high interference when better choices exist. To achieve both goals we proceed, on each time slot, as follows:

1) Assign each user the access point providing the strongest signal (strongest AP) and group the terminals with the same strongest AP.
2) For each AP group, draw randomly one user.

It is assumed that the number of users in each list is comparable. Over a long period of time this assures fairness as all users have an equal chance of being served, while precluding the possibility of choosing in the same time slot more than one user having the same "preferred" AP. More precisely, the channel matrix $\mathbf{H} = [h_{i,j}]$ obtained in every time slot is such that

$$\arg\max_j |h_{i,j}|^2 \neq \arg\max_j |h_{k,j}|^2, \quad \forall i \neq k. \qquad (15)$$

This assures that interference-prone schemes such as NC are not unfairly penalized in our comparison by particularly poor associations. In addition, users and APs are ordered so that the $k$-th AP is the smallest path-loss AP for the $k$-th user. This yields a channel matrix in which the largest magnitude element in each row lies on the main diagonal of the matrix.

The fact that the above described procedure resulted in equal likelihood of service for all users was confirmed in our simulations by verifying that when the scheduling algorithm was repeated many times, any specific choice of position received service the same number of times. While it may be possible to find scheduling algorithms that further benefit the performance of the NC scheme, it should first be verified that these gains are not achieved at the expense of fairness.

As is to be expected, unobstructed hall scenarios provide less natural isolation between AP-user pairs than aisle-to-office scenarios. This results in the fact that the hall scenarios were characterized by a significantly smaller path-loss exponent, see Table I. As a consequence, for any given distribution of distances between APs and users, the channel matrices associated with hall scenarios will tend to be less diagonally dominant, i.e., the off-diagonal terms of $\mathbf{H}$ will be larger on average. The effect of this on the rate achievable by each transmission technique will be discussed later in this section.

In all the evaluations, the noise variance in the receiver, for all full-band schemes (i.e., excluding FD), was chosen to be $-90$ dBm, which roughly corresponds to the thermal noise in a receiver with a noise figure of 10 dB, operating at room temperature, over a bandwidth of 20 MHz.

### A. Aisle-to-office Scenarios

For each aisle-to-office scenario, 500 4-by-4 channel matrices satisfying (15) were selected by randomly choosing from the set of measured channel data for the corresponding site.

The CDF of the per-user rates, attained when $\mathbf{W}$ and $\{p_k\}$ are chosen so as to maximize the sum rate in each scheme, is shown in Fig. 2 for scenario aisle-to-office 1, under the PAPC (9b) with $P = 20$ dBm. The results obtained in the other aisle-to-office scenarios were quite similar. It can be seen directly from the graph that at this transmit power limit, the three network-MIMO techniques outperform NC and FD for all availabilities. We also observe that the performance of DPC and ZF-DPC are very close, which is consistent with results obtained before for Rayleigh i.i.d. channels [10]. It should also be noted that the optimization methods used only assure that the sum capacity of DPC is the best of all coordinated systems. While this was observed in all our calculations, it does not necessarily imply that at all availability levels, the per-user rate of DPC will exceed that of the other options. In fact we found that for some users, the ZF-DPC rates would exceed those of DPC, as can be observed from the CDFs at low availabilities. At high availabilities however, DPC invariably proved to be best. As the transmit power limit is reduced, e.g. to values below -20 dBm, we found that an increasing number of users have a non-zero probability of being assigned zero rate when using DPC, ZF-DPC or ZF. This is a consequence of the fact that we are considering the per-user rates when each of the network-MIMO systems is configured for maximum sum rate, not fairness. As a consequence, the best strategy

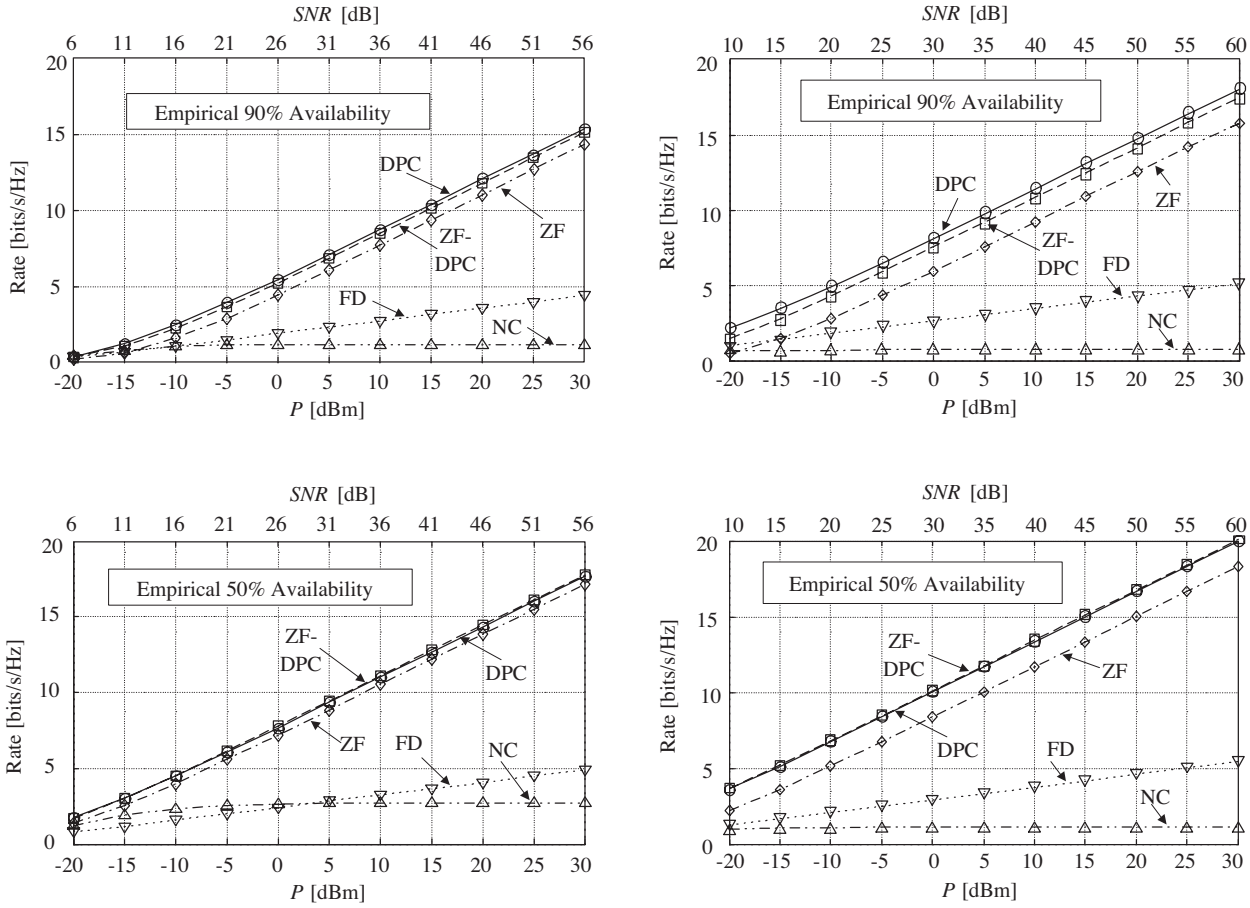


Fig. 3. User rates at different availabilities for scenarios aisle-to-office 1 (first column) and hall 2 (second column).

may include not serving some users at all in some channel realizations. This behavior will be discussed in more detail below.

The corresponding per-user rates of each scheme in aisle-to-office scenario 1, as a function of $P$, are shown in the first column of Fig. 3, for availabilities 50% and 90%. On the upper edge of each of these graphs we have included an additional horizontal axis, labeled *SNR*, to provide an algorithm-independent measure of the received signal-to-noise ratio for each site. This *SNR* corresponds to the average received *SNR* in the NC setting excluding interference (i.e., supposing interfering APs are turned off), that is

$$SNR = \frac{P}{N}\left(\frac{1}{4\times 500}\sum_{n=1}^{500}\sum_{i=1}^{4}\left|h_{i,i}^{(n)}\right|^2\right), \qquad (16)$$

where $h_{i,i}^{(n)}$ is the $i$-th diagonal entry of the $n$-th channel-matrix instantiation. This would also be the true *SNR* for all the full-band schemes considered here if the off-diagonal terms of the channel matrix were zero. Since the latter condition never holds, this notion of *SNR* is not the actual per-user signal-to-noise ratio, which is algorithm dependent. Instead, it is the average ratio of the power received by a user from its "strongest AP," to the receiver noise. This ratio depends only on the environment, specifically on the average path loss between AP-user pairs, as can be seen from (16).

Figure 3 reveals that, in scenario aisle-to-office 1 and for a power limit $P = 5$ dBm (*SNR*= 31 dB), DPC and ZF-DPC attain a data-rate gain in excess of three times, for both 50% and 90% availabilities, when compared with NC or FD. Similar gains are observed at higher power limits. In relation to this, we note that, loosely speaking, for large values of $P$, a gain over FD of at most four times would be expected, since for large values of *SNR* and assuming perfect interference cancellation, the improvement in capacity will be dominated by the ratio of transmission bandwidths used, which is 4 in our case.

For small values of $P$, the interference terms $P\sum_{m\neq k}|h_{k,m}|^2$ in (6) are small compared to the noise variance, which implies that the performance of NC is noise-limited. In the specific case of ZF, the power of some APs will be reduced below $P$ to meet the PAPC (9) while inverting the channel by choosing $\mathbf{W} = \mathbf{H}^{-1}$. The cost of such interference avoidance effort is larger than the benefit stemming from having zero interference, yielding a sum-rate smaller than that obtained with APs at full power without coordination. The poor performance in low *SNR* regimes is a well-known shortcoming of pure ZF, which can be improved upon by using regularized zero-forcing (RZF), as discussed in [48]. We illustrate this in Fig. 4 which describes in greater detail the behavior of all techniques at low power for the case of 90% availability. Under such conditions the performance improvement of RZF over ZF becomes evident. As previously discussed, it can also be seen in this figure that at low power, the objective of maximizing sum rate may be achieved by

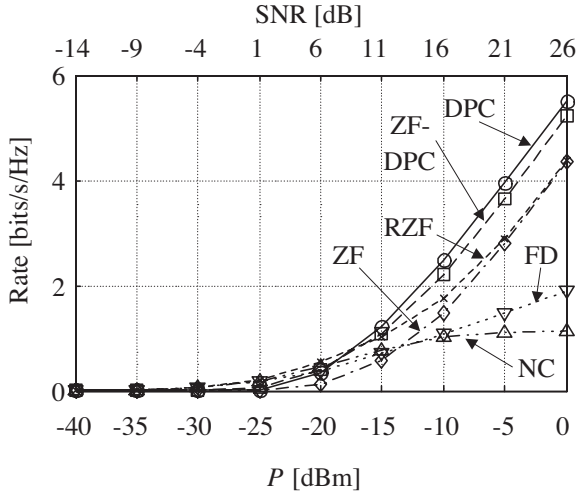


Fig. 4. User rates at 90% availability for scenarios aisle-to-office 1.

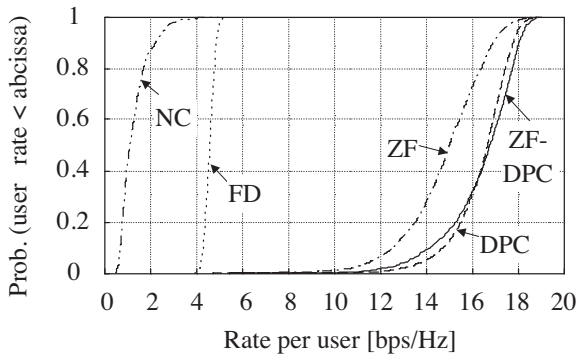


Fig. 5. CDF plots of rate per user, obtained when NC, FD, ZF, ZF-DPC and DPC achieve their maximum sum-rates, under the power constraint $P =$ 20 dBm, from empirical channel measurements taken in scenario hall 2.

not serving some users at all, and as a consequence the rate that can be guaranteed to 90% of users may drop to zero.

### *B. Hall Scenarios*

A procedure similar to the one described before was followed to generate 4-by-4 channel matrices in the two hall scenarios where measurements were taken. The CDF of the per-user rates obtained with each network-MIMO technique when optimizing for sum rate under power constraint $P = 20$ dBm are shown in Fig. 5, for scenario hall 2. In this figure we see again that the three network-MIMO techniques considered here provide higher per-user data rates than NC and FD.

The corresponding per-user rates for several availabilities as a function of $P$ for this scenario type are shown in the right column plots of Fig. 3, where scenario hall 2 has been chosen. The results for the other hall scenario are very similar and are omitted for the sake of brevity.

In this scenario, in the high SNR range, DPC and ZF-DPC attain roughly the same gain, in per-user rates over FD, as that observed in the aisle-to-office scenarios. On the other hand, in this more interference-prone environment, the NC maximum rates are significantly reduced when compared to those of the aisle-to-office scenarios, characterized by higher natural isolation between AP/user pairs.

The gain of the DPC schemes over ZF is also larger when compared to the aisle-to-office scenarios. Loosely speaking, this can be attributed to the fact that the aisle-to-office channel matrices are more diagonally dominant than the hall channel matrices. As a consequence, and in view of the Geršgorin-disc theorem [50], the determinant of $\mathbf{H}$ will, at times, be smaller in hall scenarios. Since for ZF the preprocessing matrix equals the inverse of $\mathbf{H}$, it will be possible for $\mathbf{W}$ to have larger elements in the hall scenarios. In view of the power constraint (9), this means smaller signal variances $p_k$ and thus smaller sum-rates for ZF (see (8)). In contrast, ZF-DPC is less sensitive to the smaller-determinant matrices that arise in the hall scenarios. The reason for this behaviour can be found in the fact that the determinant of $\mathbf{H}$ is equal to the product of all the diagonal elements of $\mathbf{R}$. Thus, a given decrease in the determinant of $\mathbf{H}$ will, in general, entail a smaller reduction of rate for ZF-DPC (see (13)).

As can be observed from Fig. 3, high-interference scenarios do not always result in decreased per-user rates. While this certainly occurs for a non-coordinated system as clearly seen from the graphs, DPC, ZF-DPC and to a lesser degree ZF may yield an improved performance in the hall scenarios in comparison to that obtained in the better isolated aisle-to-office environments. The improvement is particularly significant (a factor of around 2) at low power, as seen at the left extreme of the graphs. We note that the performance improvement is still evident when the comparison is carried out at equal *SNR*, i.e., when the differences in average path losses between AP/user pairs for the scenarios has been compensated. This behaviour can be explained by recalling that, at low power, noise rather than interference is the relevant factor in limiting transmission rates. Since the channel matrices of the aisle-to-office scenarios are more strongly diagonal-dominant, less power reaches a user from access points other than the one that is dominant. In contrast, in an environment with less isolation (such as the unobstructed halls), the DPC schemes can take advantage of the fact that significant power from all bases will reach each user, while managing to turn most of this power into signal, not interference. (Indeed, it can be seen from (14) that for sufficiently large noise power, increasing the magnitude of the off-diagonal elements of $\mathbf{H}$ may produce a relatively larger increase in the numerator of the fraction within the $\log(\cdot)$ than on its denominator.) Thus the signal-to-noise-plus-interference ratio is improved. As transmit power increases however, interference becomes dominant, and the hall scenarios suffer from the increased need to compensate for this impairment.

### *C. Accuracy of the channel model at predicting achievable network-MIMO rates*

In order to assess the accuracy of the log-normal plus Rayleigh/Rice model at predicting the maximum rates achievable by the techniques described in Section IV, we obtained those rates from channel matrices generated by the general model for each scenario type (aisle-to-office or hall), that is, using the parameters in the boldface rows of Table I. The data rates predicted by the model were, in general, in good agreement with those obtained from empirical data, for each scenario. Figure 6 shows plots of per-user rate with respect

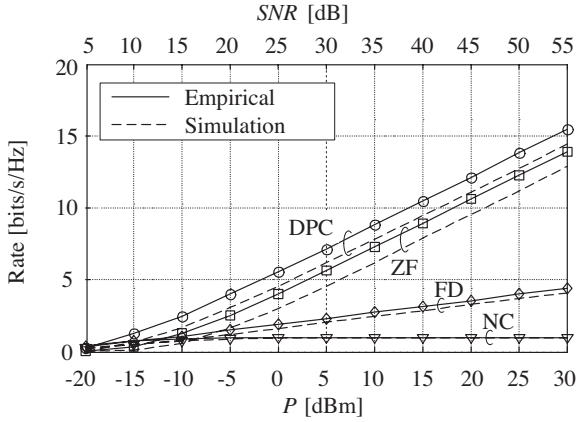


Fig. 6. 90% availability empirical and simulated per-user rates for scenario aisle-to-office 3. Simulated rates were obtained from the model using the scenario-type parameters in row "All aisle-to-office scenarios" of Table I.

to maximum transmit power constraint $P$ for 90% availability for the scenario aisle-to-office 3. It can be seen that, for this scenario, the rates from simulated channels are smaller than those obtained from empirical data. This may be attributed to the fact that the scenario-specific parameter $L_{ref}$ for aisle-to-office 3 (in the third row of Table I) is smaller than that of the corresponding general model used for the scenario type (contained in the fourth row of Table I). Thus, in this case the actual received powers will be larger (on average) than those predicted by the model.

## VI. Conclusions

In this paper we have evaluated the data rates achievable in an indoor wireless 4-by-4 system by network-MIMO techniques such as zero-forcing (ZF), zero-forcing dirty paper coding (ZF-DPC) and dirty paper coding (DPC). We compared these rates with those achievable with frequency diversity (FD) and no coordination (NC), using measured and simulated indoor channel matrices at 3.5 GHz. Our results show that a single-slope log-normal plus Rayleigh fading model with properly chosen parameters is good at predicting the sum-rate performance statistics of these techniques. By numerical evaluation based on empirical data we have shown that in the scenarios tested, at high *SNR*, the network-MIMO techniques are able to achieve about a three-fold increase in per-user data rates over NC or FD, when considering 50% and 90% availabilities. It was also found that schemes employing dirty paper coding can attain higher per-user rates in hall scenarios, where interference is greater than in aisle-to-office scenarios. This difference was greater for high availability data rates and at small *SNR*s. Our evaluations also revealed that while ZF in general provides higher data rates than NC and FD, this advantage is lost at low *SNR*, particularly when high availability is considered. In contrast, DPC based schemes provide significant benefits under virtually all practical conditions.

## Acknowledgement

The authors would like to thank Francisco Silva, Dragan Samardzija and Sivarama Venkatesan for their valuable help.

## References

[1] J. Andrews, W. Choi, and R. Heath, "Overcoming interference in spatial multiplexing MIMO cellular networks," *IEEE Wireless Commun. Mag.*, vol. 14, no. 6, pp. 95–104, Dec. 2007.

[2] G. Boudreau, J. Panicker, N. Guo, R. Chang, N. Wang, and S. Vrzic, "Interference coordination and cancellation for 4G networks," *IEEE Commun. Mag.*, vol. 47, no. 4, pp. 74–81, Apr. 2009.

[3] S. Venkatesan, A. Lozano, and R. Valenzuela, "Network MIMO: overcoming intercell interference in indoor wireless systems," in *Proc. Asilomar Conf. Signals, Systems and Computers (ACSSC 2007)*, Nov. 2007, pp. 83–87.

[4] M. Karakayali, G. Foschini, and R. Valenzuela, "Network coordination for spectrally efficient communications in cellular systems," *IEEE Wireless Commun. Mag.*, vol. 13, no. 4, pp. 56–61, Aug. 2006.

[5] M. Costa, "Writing on dirty paper (corresp.)," *IEEE Trans. Inf. Theory*, vol. 29, no. 3, pp. 439–441, May 1983.

[6] H. Weingarten, Y. Steinberg, and S. Shamai, "The capacity region of the Gaussian multiple-input multiple-output broadcast channel," *IEEE Trans. Inf. Theory*, vol. 52, no. 9, pp. 3936–3964, Sep. 2006.

[7] P. Viswanath and D. Tse, "Sum capacity of the vector Gaussian broadcast channel and uplink-downlink duality," *IEEE Trans. Inf. Theory*, vol. 49, no. 8, pp. 1912–1921, Aug. 2003.

[8] W. Yu and J. Cioffi, "Sum capacity of Gaussian vector broadcast channels," *IEEE Trans. Inf. Theory*, vol. 50, no. 9, pp. 1875–1892, Sep. 2004.

[9] G. Caire and S. Shamai, "On achievable rates in a multi-antenna Gaussian broadcast channel," in *Proc. Int. Symp. Information Theory (ISIT 2001)*, June 2001, p. 147.

[10] ——, "On the achievable throughput of a multiantenna Gaussian broadcast channel," *IEEE Trans. Inf. Theory*, vol. 49, no. 7, pp. 1691–1706, July 2003.

[11] F. Boccardi and H. Huang, "Zero-forcing precoding for the MIMO broadcast channel under per-antenna power constraints," in *Proc. IEEE Workshop Signal Processing Advances in Wireless Comm. (SPAWC 2006)*, July 2006, pp. 1–5.

[12] D. Samardzija, H. Huang, R. Valenzuela, and T. Sizer, "An experimental downlink multiuser MIMO system with distributed and coherently-coordinated transmit antennas," in *Proc. IEEE Intl. Conf. Comm. (ICC 2007)*, June 2007, pp. 5365–5370.

[13] J. Zhang, R. Chen, J. Andrews, A. Ghosh, and R. Heath, "Networked MIMO with clustered linear precoding," *IEEE Trans. Wireless Commun.*, vol. 8, no. 4, pp. 1910–1921, Apr. 2009.

[14] A. L. Stolyar and H. Viswanathan, "Self-organizing dynamic fractional frequency reuse in OFDMA systems," in *Proc. IEEE Infocom*, Apr. 2008, pp. 1364–1372.

[15] M. C. Necker, "Local interference coordination in cellular OFDMA networks," in *Proc. IEEE Veh. Technol. Conf. (VTC 2007-Fall)*, Oct. 2007, pp. 1741–1746.

[16] S. Venkatesan, "Coordinating base stations for greater uplink spectral efficiency in a cellular network," in *Proc. IEEE PIMRC*, Sep. 2007.

[17] ——, "Coordinating base stations for greater uplink spectral efficiency: proportionally fair user rates," in *Proc. IEEE PIMRC*, Sep. 2007.

[18] H. Huang, M. Trivellato, A. Hottinen, M. Shafi, P. J. Smith, and R. Valenzuela, "Increasing downlink cellular throughput with limited network MIMO coordination," *IEEE Trans. Wireless Commun.*, vol. 8, no. 6, pp. 2983–2989, June 2009.

[19] S. Venkatesan, H. Huang, Á. Lozano, and R. Valenzuela, "A WiMAX-based implementation of network MIMO for indoor wireless systems," *EURASIP J. Advances in Signal Process.*, vol. 2009, 2009, article ID 963547.

[20] A. Wyner, "Shannon-theoretic approach to a Gaussian cellular multiple-access channel," *IEEE Trans. Inf. Theory*, vol. 40, no. 6, pp. 1713–1727, Nov. 1994.

[21] S. Shamai and A. Wyner, "Information-theoretic considerations for symmetric, cellular, multiple-access fading channels." *IEEE Trans. Inf. Theory*, vol. 43, no. 6, pp. 1877–1894, Nov. 1997.

[22] O. Somekh and S. Shamai, "Shannon-theoretic approach to a Gaussian cellular multiple-access channel with fading," *IEEE Trans. Inf. Theory*, vol. 46, no. 4, pp. 1401–1425, July 2000.

[23] S. Shamai and B. Zaidel, "Enhancing the cellular downlink capacity via co-processing at the transmitting end," in *Proc. IEEE Veh. Technol. Conf. (VTC 2001-Spring)*, vol. 3, May 2001, pp. 1745–1749.

[24] O. Somekh, O. Simeone, Y. Bar-Ness, and A. Haimovich, "Cth11-2: distributed multi-cell zero-forcing beamforming in cellular downlink channels," in *Proc. IEEE Global Telecomm. Conf. (GLOBECOM)*, Dec. 2006, pp. 1–6.

[25] O. Somekh, B. Zaidel, and S. Shamai, "Sum rate characterization of joint multiple cell-site processing," *IEEE Trans. Inf. Theory*, vol. 53, no. 12, pp. 4473–4497, Dec. 2007.
[26] O. Somekh, O. Simeone, A. Sanderovich, B. Zaidel, and S. Shamai, "On the impact of limited-capacity backhaul and inter-users links in cooperative multicell networks," in *Proc. Annual Conf. on Information Sciences and Systems (CISS 2008)*, Mar. 2008, pp. 776–780.
[27] A. Sanderovich, O. Somekh, and S. Shamai, "Uplink macro diversity with limited backhaul capacity," in *Proc. Int. Symp. Information Theory (ISIT 2007)*, June 2007, pp. 11–15.
[28] P. Marsch and G. Fettweis, "A framework for optimizing the uplink performance of distributed antenna systems under a constrained backhaul," in *Proc. IEEE Intl. Conf. Comm. (ICC 2007)*, June 2007, pp. 975–979.
[29] J. Weitzen and T. Lowe, "Measurement of angular and distance correlation properties of log-normal shadowing at 1900 MHz and its application to design of PCS systems," *IEEE Trans. Veh. Technol.*, vol. 51, no. 2, pp. 265–273, Mar. 2002.
[30] E. Perahia, D. Cox, and S. Ho, "Shadow fading cross correlation between basestations," in *Proc. IEEE Veh. Technol. Conf. (VTC 2001-Spring)*, vol. 1, May 2001, pp. 313–317.
[31] V. Graziano, "Propagation correlations at 900 MHz," *IEEE Trans. Veh. Technol.*, vol. 27, no. 4, pp. 182–189, Nov. 1978.
[32] N. Jaldén, P. Zetterberg, B. Ottersten, and L. García, "Inter- and intrasite correlations of large-scale parameters from macrocellular measurements at 1800 MHz," *EURASIP J. Wireless Commun. and Networking*, 2007.
[33] N. Jaldén, P. Zetterberg, B. Ottersten, A. Hong, and R. Thoma, "Correlation properties of large scale fading based on indoor measurements," in *Proc. IEEE Wireless Commun. Networking Conf. (WCNC 2007)*, Mar. 2007, pp. 1894–1899.
[34] M. Denis, V. Vasudevan, K. Chandra, and C. Thompson, "Characterizing spatial correlation in indoor channels," in *Proc. IEEE Wireless Commun. Networking Conf. (WCNC 2004)*, vol. 3, Mar. 2004, pp. 1850–1855.
[35] T. S. Rappaport, *Wireless Communications: Principles and Practice*, 2nd edition. Upper Saddle River, NJ: Prentice-Hall, 2002.
[36] J. Andersen, T. Rappaport, and S. Yoshida, "Propagation measurements and models for wireless communications channels," *IEEE Commun. Mag.*, vol. 33, no. 1, pp. 42–49, Jan. 1995.
[37] S. Phaiboon, "An empirically based path loss model for indoor wireless channels in laboratory building," in *Proc. IEEE TENCON*, vol. 2, Oct. 2002, pp. 1020–1023.
[38] C. Oestges, D. Vanhoenacker-Janvier, and B. Clerckx, "Channel characterization of indoor wireless personal area networks," *IEEE Trans. Antennas Propag.*, vol. 54, no. 11, pp. 3143–3150, Nov. 2006.
[39] T. A. Wysocki and H.-J. Zepernick, "Characterization of the indoor radio propagation channel at 2.5 GHz," *J. Telecommun. and Inf. Technnol.*, vol. 3-4, pp. 84–90, 2000.
[40] A. Chandra, A. Kumar, and P. Chandra, "Comparative study of path losses from propagation measurements at 450 MHz, 900 MHz, 1.35 GHz and 1.89 GHz in the corridors of a multifloor laboratory-cum-office building," in *Proc. IEEE Veh. Technol. Conf. (VTC 1999-Fall)*, vol. 4, Sep. 1999, pp. 2272–2276.
[41] H. Zaghloul, G. Morrison, and M. Fattouche, "Frequency response and path loss measurements of indoor channel," *Electron. Lett.*, vol. 27, no. 12, pp. 1021–1022, June 1991.
[42] S. Guérin, Y. J. Guo, and S. K. Barton, "Indoor propagation measurements at 5 GHz for HIPERLAN," in *Proc. Int. Conf. Antennas and Propagation*, Apr. 1997, Conf. Publication No. 436.
[43] A. Goldsmith, *Wireless Communications*. New York: Cambridge University Press, 2005.
[44] R. J. C. Bultitude, R. F. Hahn, and R. J. Davies, "Propagation considerations for the design of an indoor broad-band communications system at EHF," *IEEE Trans. Veh. Technol.*, vol. 47, no. 1, pp. 235–245, Feb. 1998.
[45] P. Kyösti, J. Meinilä, L. Hentila, X. Zhao, T. Jämsä, C. Schneider, M. Narandzić, M. Milojević, A. Hong, J. Ylitalo, V.-M. Holappa, M. Alatossava, R. Bultitude, Y. de Jong, and T. Rautiainen, "D1.1.2 WINNER II channel models–part I: channel models," WINNER Information Society Technologies, Tech. Rep. IST-4-027756 WINNER II, version 1.2, Sep. 2007.
[46] A. Wiesel, Y. Eldar, and S. Shamai, "Zero-forcing precoding and generalized inverses," *IEEE Trans. Signal Process.*, vol. 56, no. 9, pp. 4409–4418, Sep. 2008.
[47] S. Boyd and L. Vandenberghe, *Convex Optimization*. Cambridge, UK: Cambridge University Press, 2004.
[48] C. Peel, B. Hochwald, and A. Swindlehurst, "A vector-perturbation technique for near-capacity multiantenna multiuser communication–part I: channel inversion and regularization," *IEEE Trans. Commun.*, vol. 53, no. 1, pp. 195–202, Jan. 2005.
[49] D. Samardzija and N. Mandayam, "Multiple antenna transmitter optimization schemes for multiuser systems," in *Proc. IEEE Veh. Technol. Conf. (VTC 2003-Fall)*, vol. 1, Oct. 2003, pp. 399–403.
[50] R. A. Horn and C. R. Johnson, *Matrix Analysis*. Cambridge, UK: Cambridge University Press, 1985.
[51] S. Vishwanath, N. Jindal, and A. Goldsmith, "Duality, achievable rates, and sum-rate capacity of Gaussian MIMO broadcast channels," *IEEE Trans. Inf. Theory*, vol. 49, no. 10, pp. 2658–2668, Oct. 2003.
[52] W. Yu and T. Lan, "Transmitter optimization for the multi-antenna downlink with per-antenna power constraints," *IEEE Trans. Signal Process.*, vol. 55, no. 6, part 1, pp. 2646–2660, June 2007.

**Rodolfo Feick** (S'71-M'76-SM'95) obtained the degree of Ingeniero Civil Electrónico at Universidad Técnica Federico Santa María, Valparaíso, Chile in 1970 and the Ph.D. degree in Electrical Engineering at the University of Pittsburgh in 1975.

He has been with the Department of Electronics Engineering at Universidad Técnica Federico Santa María since 1975, where he is currently an Associate Researcher. His current interests include RF channel modeling, digital communications, microwave system design and RF measurement.

**Milan S. Derpich** (S'08-M'09) received the Ingeniero Civil Electrónico degree from the Universidad Técnica Federico Santa María (UTFSM), Valparaíso, Chile in 1999. During his time at the university he was supported by a full scholarship from the alumni association and upon graduating received several university-wide prizes. Mr. Derpich also worked by the electronic circuit design and manufacturing company Protonic Chile S.A. between 2000 and 2004. In 2009 he received the Ph.D. degree in electrical engineering from the University of Newcastle, Australia. He received the Guan Zhao-Zhi Award at the Chinese Control Conference 2006, and the Research Higher Degrees Award from The Faculty of Engineering and Built Environment, University of Newcastle, Australia, for his PhD thesis. Since 2009 he has been with the Electonic Engineering Department at Universidad Técnica Federico Santa María, Chile. His main research interests include communications, rate-distortion theory, networked control systems, sampling and quantization.

**Reinaldo A. Valenzuela** (M'85-SM'89-F'99) Obtained his B.Sc. at the University of Chile, and his Ph.D. from Imperial College of Sc. and Tech., U. of London, England. At Bell Laboratories, he carried out indoor microwave propagation measurements and developed statistical models. He also worked on packet reservation multiple access for wireless systems and optical WDM networks. He became Manager, Voice Research Dept., at Motorola Codex, involved in the implementation integrated voice and data packet systems. On returning to Bell Laboratories he was involved in propagation measurements and ray tracing propagation prediction. He received the Distinguished Member of Technical Staff award and is Director of the Wireless Communications Research Department. He is currently engaged in MIMO / space time systems achieving high capacities using transmit and receive antenna arrays. He is a Fellow of the IEEE. He has been editor for the IEEE TRANSACTIONS ON COMMUNICATIONS and IEEE TRANSACTIONS ON WIRELESS COMMUNICATIONS. He has published over 130 papers and has 12 patents. He has over 10000 Google Scholar citations and he is a "Highly Cited Author" In Thomson ISI and a Fulbright Senior Specialist. He is the 2010 recipient of the IEEE Eric E. Sumner Award.

**Héctor Carrasco** received the Ingeniero Civil Electrónico degree from the Universidad Técnica Federico Santa María (UTFSM), Valparaíso, Chile, and the PhD in Telecommunications Engineering degree from Universidad Politécnica de Cataluña, Spain. His research interests include wireless communications, antennas, digital communications, microwave systems and satellite communications.

**Luciano Ahumada** (S'04-M'07) obtained the degree of Ingeniero Civil Electrónico at Universidad Técnica Federico Santa María, Valparaíso, Chile in 2003, and the Doctor in Electronics Engineering degree from the Universidad Técnica Federico Santa María, Chile in 2005. He has been working since March 2005 at the Escuela de Ingeniería Informática, Universidad Diego Portales, Santiago, Chile. His research interests include the performance analysis of wireless systems and data communications.

**Howard Huang** received a BSEE degree from Rice University in 1991 and a Ph.D. in electrical engineering from Princeton University in 1995. Since then, he has been a researcher at Bell Labs, in Holmdel, New Jersey, currently as a Distinguished Member of Technical Staff in the wireless access domain of Alcatel-Lucent. His research interests include wireless communication theory and cellular system design. He has taught as an adjunct professor at Columbia University and is a Senior Member of the IEEE.

**Chris T. K. Ng** (S'99–M'07) received the B.A.Sc. degree in engineering science from the University of Toronto, Toronto, ON, Canada. He received the M.S. and Ph.D. degrees in electrical engineering from Stanford University, Stanford, CA. Since 2009, he has been a Member of Technical Staff at Bell Labs, Alcatel-Lucent, in Holmdel, NJ. From 2007 to 2008, he was a Postdoctoral Researcher in the Department of Electrical Engineering and Computer Science at the Massachusetts Institute of Technology, Cambridge, MA. His research interests include cooperative communications, joint source-channel coding, cross-layer wireless network design, optimization, and network information theory. Dr. Ng was a recipient of the 2007 IEEE International Symposium on Information Theory Best Student Paper Award, and a recipient of a Croucher Foundation Fellowship in 2007.

**Pablo Arancibia** was born in Viña del Mar, Chile, in 1984. He obtained the Ingeniero Civil Electrónico and the MSc. in Electronics Engineering degree from Universidad Técnica Federico Santa María, Chile in 2010. His researches interests are in wireless communications. He currently works by Defontana in Santiago as a networking engineer.